A study on the flow characteristics of the ramp tabs with installed location

2008. 10. 19

Kim Kyoung Rean

Table of contents

1. INTRODUCTION

Methods for controlling the flight attitude of an aircraft can be broadly divided into aerodynamic control and thrust vector control. Utilizing the aerodynamic force generated from the surface of an aircraft or the control surface of its wings, aerodynamic control is directly correlated to the amount of aerodynamic force. For this reason, flight attitude control abilities are reduced in areas where the aircraft's pace is slow or air is scarcely present.[1] On the other hand, thrust vector control directly deviates thrust and gains power to control the aircraft's direction. It operates regardless of whether there exists air; it is also possible to steeply turn the aircraft at the initial stage of launch.

Thrust vector control can be classified into mechanical and aerodynamic methods. The mechanical method utilizes mechanical deflectors such as ramp tabs, jet vanes, and jetaveta, while the aerodynamic method controls thrust by ejecting secondary injection gas from inside a nozzle and causing bow shock and flow separation. When conducting thrust vector control on a ramp tab, a type of mechanical deflector, flow separation is not induced within the nozzle—as in the case of secondary injection gas—and ramp tabs are installed at the outlet of the supersonic nozzle instead to generate normal shock and oblique shock inside the ramp tabs and set off high voltage in this area.

Christopher developed a mathematical model of a one-dimensional flow field to predict the location of normal shock generated from inside the ramp tabs. He did not, however, conduct research on the control force affecting the ramp tabs, which is essential for performing thrust vector control.[4] Leslie identified the structures of shock generated within the ramp tabs by the amount of ramp tabs used.[5] In conducting their experiment, Deans et al. installed ramp tabs and jet vanes on the outlet of the supersonic nozzle so that they could control the levels of pitching, rolling, and thrust of the aircraft.

Installing ramp tabs symmetrically and asymmetrically, this study seeks to identify aerodynamic features by understanding flow phenomena appearing in and out of the ramp tabs. The control force, thrust spoilage, and thrust deviation angle affecting the ramp tabs are also analyzed in an effort to suggest a new direction for designing thrust vector control systems.

2. EXPERIMENT DEVICES AND METHODS

2.1 Supersonic Flow Test Equipment

Supersonic flow test equipment is used to pressurize and store high-pressure air, turn on the on-off valve, and eject compressed air through the supersonic nozzle within a second to generate supersonic flow. As shown in Fig. 1, this equipment consists of a pressurizing system, storage container, control valve, chamber, nozzle, and measurement equipment.

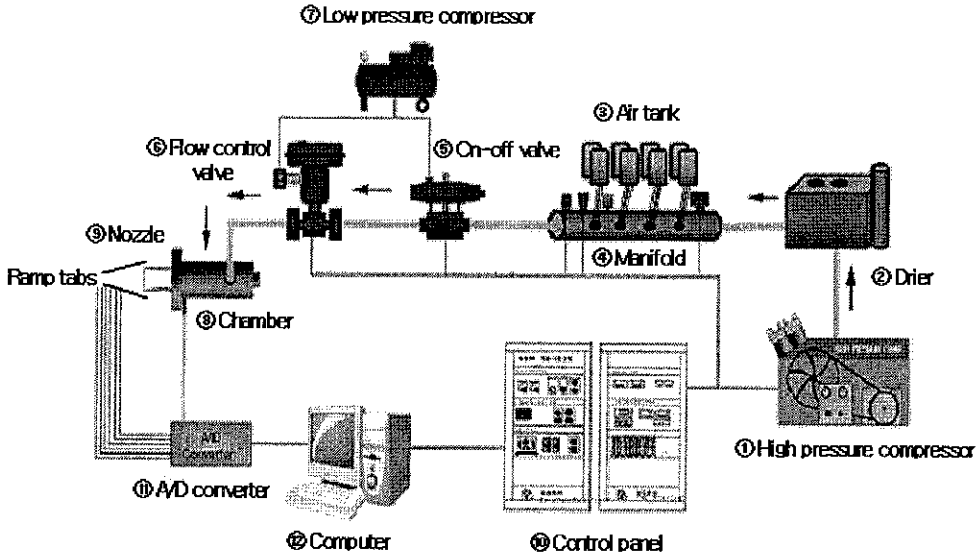

Fig. 1 Schematic diagram of experimental apparatus

The pressurizing system is composed of a high-pressure compressor and a drier. The high-pressure compressor is a reciprocating device with a maximum

opening pressure of 34.32㎫ and a stroke volume of 475 l/min. After the air is compressed by the high-pressure compressor, freezing and desiccant driers are used to eliminate moisture in the air and thereby reduce possible measurement errors in the flow simulation test.

The storage container has 16 high-pressure air tanks with an allowable pressure of 14.7㎫ and two large-capacity air tanks (450l for each); it also includes a 76l manifold with an allowable pressure of 19.61㎫. Its total storage capacity is 2064l. [2]

2.2 Thrust Vector Control Equipment

Fig. 2 shows the outline of a device for testing the performance of ramp tab thrust vector control equipment. The device is comprised of a single-component load cell, a chamber, a supersonic nozzle, a ramp tab, a six-component load cell, a housing, and a support component.

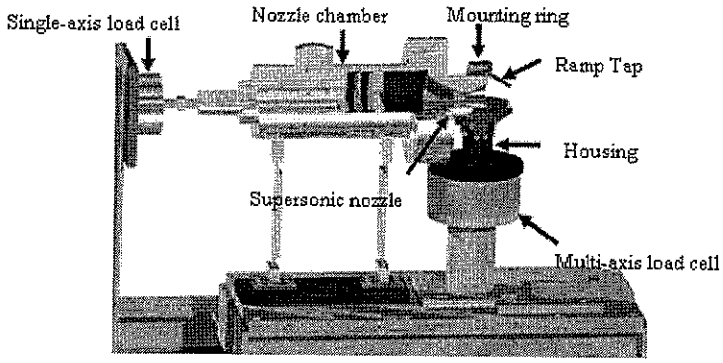

Fig. 2 Experimental apparatus for thrust vector control

As the thrust of the rocket nozzle propeller generates the repulsive force of gas ejected at high temperature, pressure, and speed, the single-component load cell measures the relevant thrust performance and component. As illustrated in Fig. 2, three ramp tabs are installed, at 120-degree intervals, on the outlet of the supersonic nozzle. The housing, which binds the ramp tabs, is installed on the six-component

load cell, which measures forces affecting each direction (i.e. ±Fx, ±Fy, ±Fz) and moment (i.e. ±Mx, ±My, ±Mz); the supporting part is movable back and forth as the length of the nozzle changes.

The ramp tab is set to be movable to the radial direction following the nozzle axis so that it can vary the diameter of the ramp tab outlet. Thus, any change in the diameter of the ramp tab outlet can modify the direction of the aircraft depending on the location of shock and the change in control force.

2.3 Experiment Models and Conditions

A ramp tab is exposed to high-pressure, high-speed nozzle flow, and hence faces considerable thermal and aerodynamic loads depending on its shape and location. Therefore, it is necessary to take into consideration the design factors of the ramp tab according to different nozzle diameters. Fig. 3 demonstrates the design factors of a ramp tab installed on a supersonic nozzle outlet. Considering factors that determine the area of the ramp tab—namely, width (W) and length (L), slope angle (), taper half angle (), area ratio (B), outlet diameter (Do), and number of tabs—the lift force should be large and the drag force and moment small. Area ratio (B) is defined by the area ratio of the ramp tab against the total wall area.

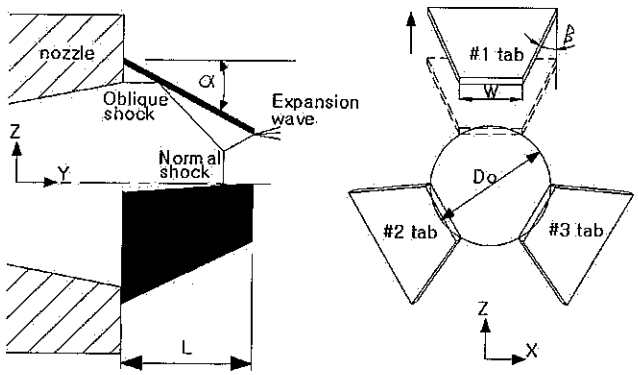

Fig. 3 Dimensional design of the ramp tab for thrust vector control

To analyze how the taper half angle of the ramp tab affects the flow field, the experiment models of the ramp tab were designed and fabricated to have taper half angles of 5 and 14. Changes in the taper half angle of the ramp tab may alter the area ratio, and therefore the location of oblique shock, the thrust deviation angle, and the thrust spoilage can be identified.

Fig. 4 presents the shape of the ramp tabs installed symmetrically and asymmetrically. In Model A, ramp tabs are installed symmetrically, and ramp tabs Nos. 1-3 move vertically at identical intervals, with the axis of the nozzle as the basis. In asymmetrical Model B, ramp tabs Nos. 2 and 3 are fixed symmetrically, and ramp tab No. 1 is set to be movable up and down, with the nozzle axis as the basis.

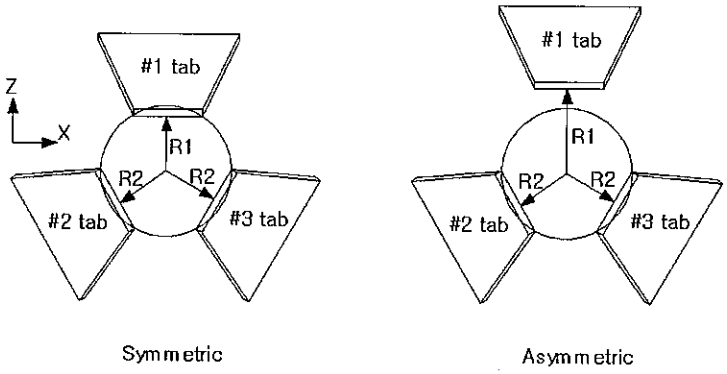

Fig. 4 Ramp tab insertion scheme for symmetric and asymmetric configuration

Design factors of the ramp tabs and the measurement of each model are shown in Fig. 3 and Table 1.

Table 1 Design parameters of ramp tab

Model	α (°)	βc (°)	R1	R2	N	L (㎜)	W (㎜)
A	25	5	Symmetrical	Symmetrical	1,2,3	60	19.45
	25	14					
B	25	5	Asymmetrical	Symmetrical	1,2,3	60	19.45
	25	14	Asymmetrical	Symmetrical			

3. EXPERIMENT RESULTS AND IMPLICATIONS

3.1 Model A

The mach number of the supersonic nozzle used in this study is 2.88; its under-expansion ratio is set to be 1.5. Fig. 5 compares and diagrams the results visualizing the flow, using a shadow graph device, to identify the structure of shock waves generated around the ramp tabs at aslope angle of 25°. Light reflections and moisture have not been entirely removed, and images gained from flow visualization were not accurate, but it has been possible to identify the structure of shock waves and the factors having predominant impacts.

Eight units of static pressure prove—used for measuring pressure—are installed in ramp tab No. 1; the numerical order of the static pressure probes are defined based on the horizontal direction starting from the outlet of the supersonic nozzle. Thus, the static pressure probe installed nearest to the supersonic nozzle is No. 1, and that installed at the end of the ramp tab is No. 8.

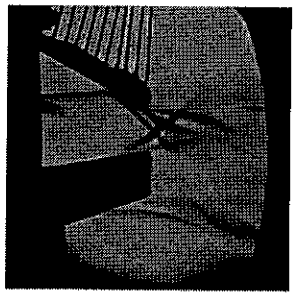

(a) R1, R2 = 21㎜

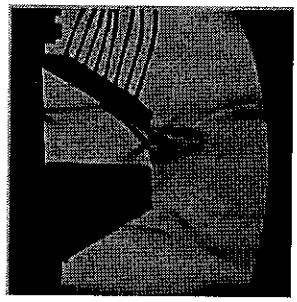

(b) R1, R2 = 21㎜

Fig. 5 Schlieren photographs of symmetrically installed ramp tabs

Fig. 5(a) is a picture of the flow field when R1, R2 = 21㎜ and the taper half angle is 5. Ejected from the supersonic nozzle, the flow is hindered by the obstacles of the ramp tabs, generating oblique shock. Between the surfaces of rear ramp tabs located on static pressure probe No. 6, the oblique shock is reflected in a

multiple manner and creates a shear layer, which, along with speed discontinuity, separates the flow generated by oblique shock.

Fig. 5(b) is a picture of the flow when R1, R2 = 21㎜ and the taper half angle is 14. Oblique shock is generated at static pressure probe No. 6. Weak normal shock is generated downstream of the ramp tabs; as the shock occurs in their downstream, it does not have significant impact on the force of the ramp tabs.

Another important factor that determines the performance of an aircraft is the drag and lift affecting the aircraft. The drag and lift coefficients acting on the ramp tabs can be derived based on the following equations:

$$C_D = \frac{D}{\frac{1}{2}\rho A V^2} \tag{1}$$

$$C_L = \frac{L}{\frac{1}{2}\rho A V^2} \tag{2}$$

where C_D is the drag coefficient, C_L the lift coefficient, A the area of the ramp tabs, ρ the density, and V the speed at the outlet of the supersonic nozzle.

Fig. 6 shows the drag and lift coefficients affecting the ramp tabs depending on changes in the taper half angle. When the taper half angle is 14 and R1=17, the drag coefficient is 0.33, 1.5 times greater than when the taper half angle is 5. This is because the greater the taper half angle becomes, the more it affects the pressure drag. At a taper half angle of 5°, the lift coefficient remains constant regardless of change to R1 when the taper half angle is 14°, however, the lift coefficient increases in proportion to R1, as an increase in the area ratio generates normal shock.

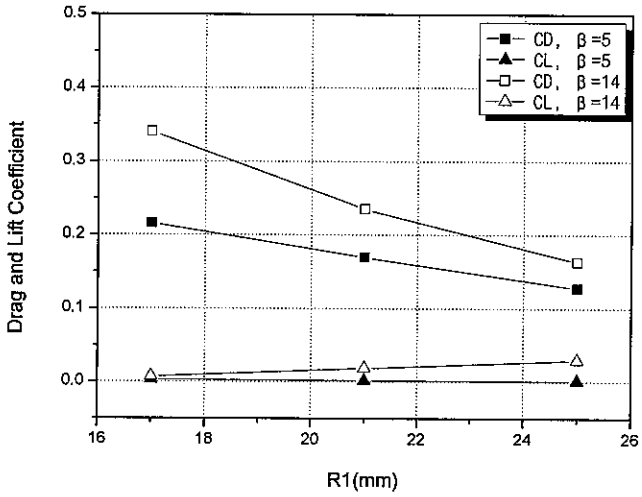

Fig. 6 Drag and Lift coefficient with the R1 variation

When installed on the outlet of the supersonic nozzle, ramp tabs deviate the flow, generating shock and deviating thrust. Thrust spoilage is caused when the ramp tabs, i.e., mechanical deflectors, are exposed.

Fig. 7 illustrates the thrust spoilage caused by ramp tabs. Thrust spoilage declines dramatically as R1 increases, values in a range of 5.1-9% are obtained at a ramp tab taper half angle of 5° and 6.7-14.1% at 14°. When the ramp tab's taper half angle is 5° and R1=21, the thrust spoilage is approximately 7.1%; when the taper half angle is 14° and R1=21, it amounts to 9.9%—about 1.4 times greater than when the angle is 20°. These results can be explained as follows: when the taper half angle increases, the larger flow contact surface and cohesion of the ramp tabs have a relatively greater impact.

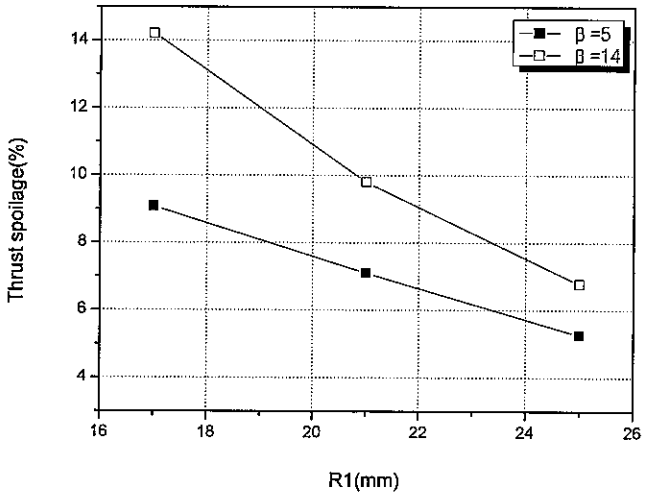

Fig. 7 Thrust spoilage in accordance with R1 variation

The high-turning capacity of thrust vector control is based only on thrust, and hence it is necessary to consider the size of thrust generated by thrust vector control devices and the thrust deviation angle.

Here the thrust deviation angle can be derived, as in Equation (3), based on the ratio of the axis-direction thrust F_a, which takes thrust spoilage into account, and the side force F_S.

$$\phi = \tan^{-1}(\frac{F_S}{F_a}) \tag{3}$$

Fig. 8 shows the respective thrust deviation angles for the ramp tab taper half angles of 5° and 14°. At a taper half angle of 5°, the thrust deviation angle approaches 0°regardless of changes in R1. At 14°, the angle increases slightly as R1 becomes larger.

Generated by the supersonic nozzle, shock collides with ramp tabs and causes an increase in the level of pressure. This does not have a significant impact on the entire thrust, as forces affecting the ramp tabs, which are installed

symmetrically, are offset in a symmetrical manner. The thrust deviation angle increases the taper half angle hence, increasing it does not necessarily translate into better performance. In other words, the taper half angle of the ramp tabs should be selected properly in order to generate a thrust deviation angle that is appropriate to the designer's aims.

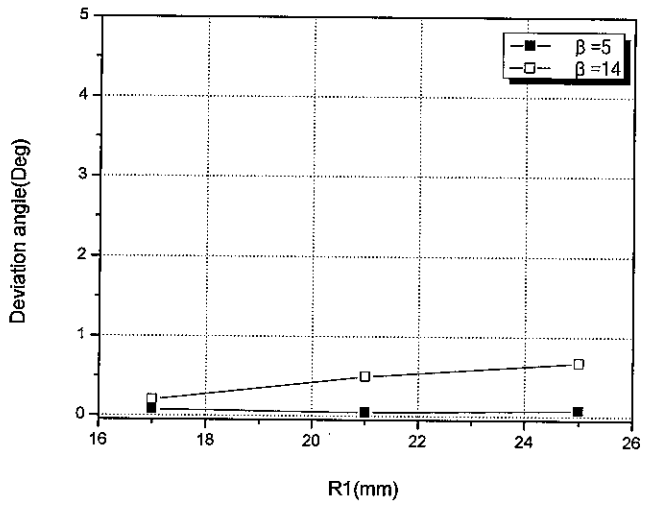

Fig. 8 Thrust deviation angle in accordance with R1 variation

3.2 Model B

Fig. 9 shows a picture of the flow field generated when ramp tab No. 1 is installed asymmetrically and ramp tabs Nos. 2-3 are installed symmetrically. In Fig. 9(a), oblique shock generated from ramp tab No. 1 flows out of the interior of the rear ramp tab, which is located in static pressure probe No. 6. Regarding oblique shock waves generated in ramp tabs Nos. 2 and 3, their exact location cannot be identified, because they are obstructed by the ramp tabs. As illustrated in Fig. 9(a), however, they are generated somewhere before static pressure probe No. 6. Oblique shock waves generated in ramp tabs Nos. 1-3 do not cross each other at the central line of the ramp tabs. However, they do cross near ramp tab No. 1, as the ramp tabs involved are installed asymmetrically. In Fig. 9(b), oblique shock generated

from ramp tab No. 1 is located in static pressure probe No. 6. However, oblique shock waves generated in ramp tabs Nos. 2-3 do move toward the downstream of the ramp tabs, as the outlet diameter of the ramp tabs is increased. Also, these oblique shock waves do not collide with the end of ramp tab No. 1, because ramp tabs Nos. 2-3 are at greater vertical distance from the center of the supersonic nozzle outlet.

In Fig. 9(c), it is seen that the area of the ramp tabs increases as their taper half angle becomes larger. Compressed within the ramp tabs, oblique shock generates reflection shock, a shear layer, and normal shock as it moves downstream. Control force is believed to increase due to normal shock generated within the ramp tabs.

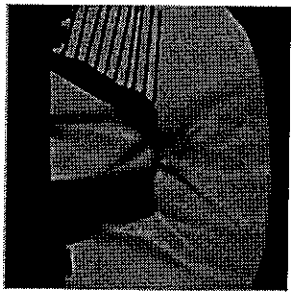

(a) R1=21, R2 = 11㎜

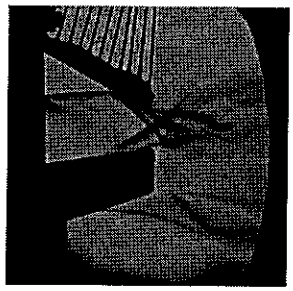

(b) R1=21, R2 = 17㎜

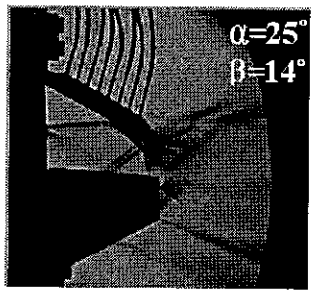

(c) R1=21, R2 = 11㎜

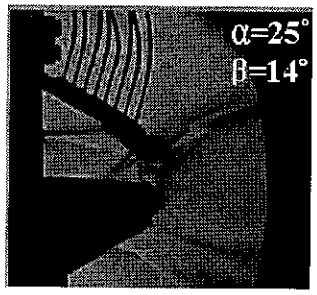

(d) R1=21, R2 = 17㎜

Fig. 9 Schlieren photograph of asymmetrically installed ramp tabs

Generated in ramp tabs Nos. 1-3, respectively, the three waves of normal shock cross each other and slip to the downstream of the ramp tabs. Flowing on

the surface of the ramp tabs, the flow generates multiple expansive waves at the end of the ramp tabs. As it moves completely beyond the ramp tabs, the flow generates a complicated, web-shaped structure of a shock wave in the downstream, with normal shock, a shear layer, and multiple expansive waves crossing each other.

Fig. 10 shows the drag and lift coefficients affecting ramp tabs in accordance with changes in R2 and the taper half angle. At a taper half angle of 14°, the drag coefficient increases by around 30% compared to when the taper half angle is 5°. As the taper half angle of ramp tabs increases, the area vertically contacting the flow expands, and the drag coefficient affecting the ramp tabs also increases sharply. The drag coefficient has significant impact on symmetrically-installed ramp tabs; it does not decline dramatically as R1 increases. In contrast, the lift coefficient has greater impact when R1 is increased. When the taper half angle is 14°and R1=25, the lift coefficient suddenly increases compared to when the angle is 5°. This is believed to be because the force of lift increases as normal shock is generated within the ramp tabs. When R2 increases, the flow ejected from the supersonic nozzle does not remain stagnant within the ramp tabs, immediately slipping out of them instead. For this reason, the drag and lift coefficients, when R2=17, exert smaller force on the ramp tabs and are less than when R2=11.

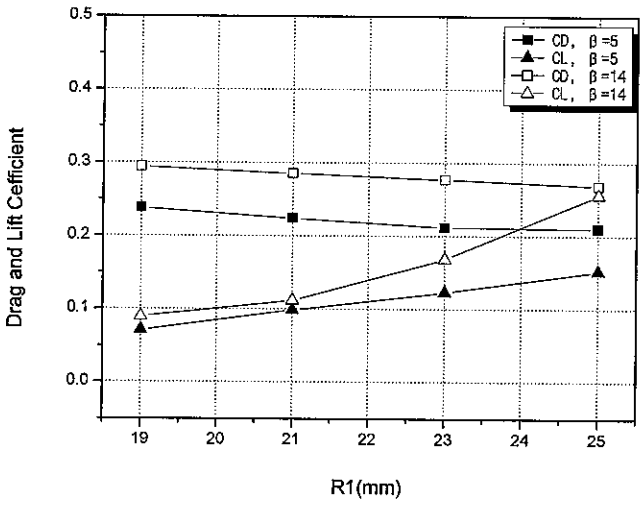

(a) R2 = 11

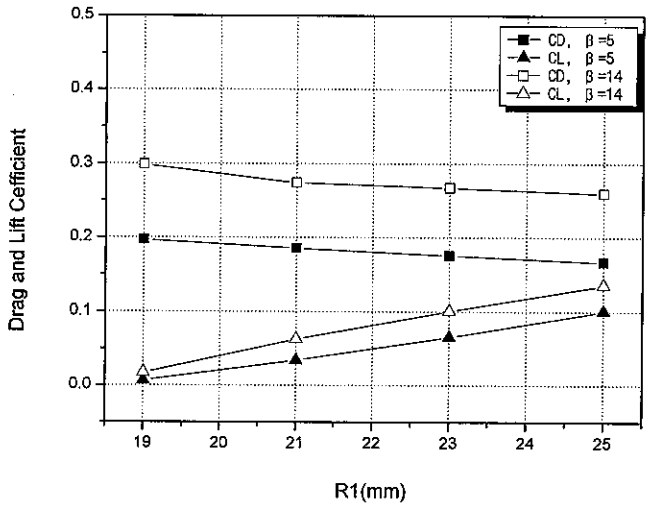

(b) R2 = 17

Fig. 10 Drag and lift coefficient in accordance with R1 variation

Fig. 11 represents the thrust spoilage generated in the ramp tabs. When the taper half angle is 5° and R2=11, the thrust spoilage sharply declines as R1 increases values in a range of 8.9-10%are obtained when R2=17, the values range from 6.8-8.1%. If ramp tabs are installed asymmetrically at the outlet of the supersonic nozzle, a decrease in R1 and R2 increases the area ratio and the drag toward the Y direction, thereby generating considerable thrust spoilage.

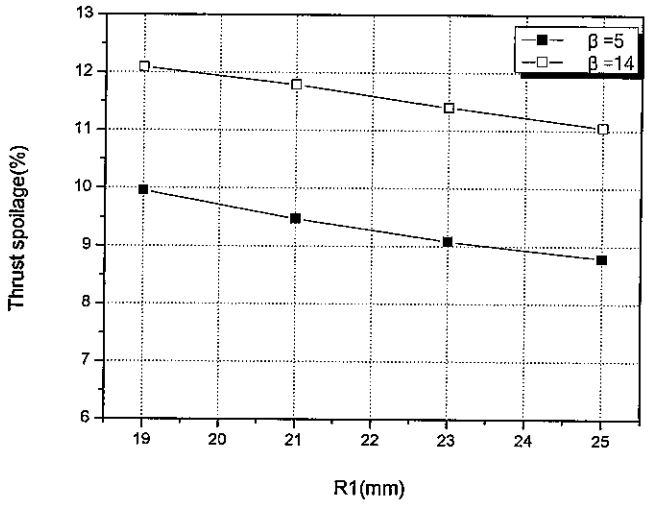

(a) R2 = 11

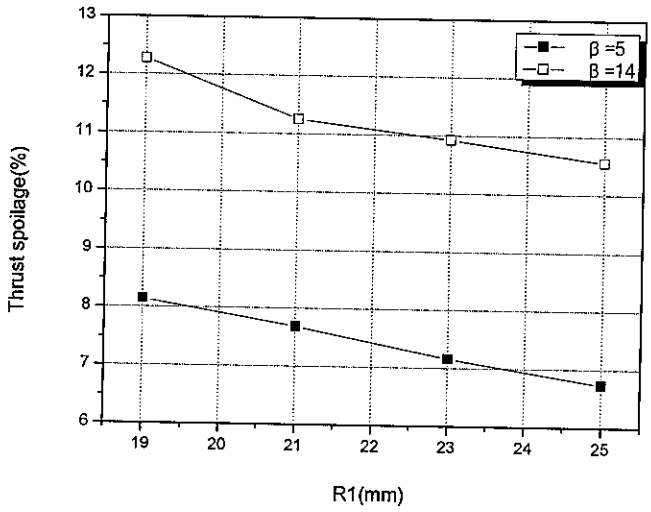

(b) R2 = 17

Fig. 11 Thrust spoilage in accordance with R1 variation

As shown in Fig. 11, when the taper half angle is extremely large, the flow area of the ramp tabs increases, and significant thrust spoilage is generated. Against this backdrop, this study seeks to identify the maximum deviation angle and control force, considering thrust spoilage generated by changes in the diameter of ramp tabs and taper half angle.

The thrust deviation angle is illustrated in Fig. 12. At a taper half angle of 5°, the thrust deviation angle tends to be linearly proportionate, within a range of 0-2.5°, to R1 of the ramp tabs. As R1 of the ramp tabs increases, the thrust deviation angle becomes proportionately larger when R2=11 and the taper half angle is 14°, the thrust deviation angle is 30-35% greater than when the taper half angle is 5°. When R2=17, the angle is smaller than when R1=11. This is because, as the outlet diameter of the ramp tabs is increased, normal shock is generated outside the ramp tabs, failing to stimulate side force.

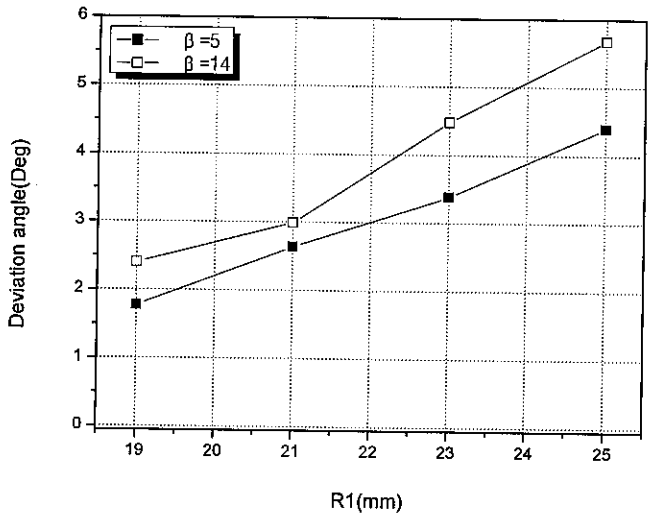

(a) R2 = 11

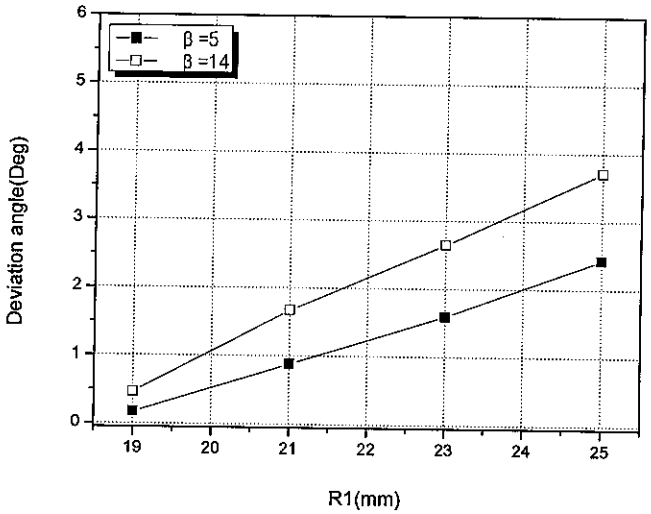

(b) R2 = 11

Fig. 12 Thrust deviation angle in accordance with R1 variation

4. CONCLUSION

This study has conducted various experiments with ramp tabs, devices for enhancing thrust vector control over the direction of an aircraft, installed

symmetrically and asymmetrically on the outlet of a supersonic nozzle. The following conclusions have been derived:

(a) The drag coefficient tends to increase dramatically when the taper half angle of ramp tabs is increased, as the area that vertically contacts the flow increases. The lift coefficient rises when R1 increases due to normal shock generated within the ramp tabs.

(b) When the ramp tabs are installed symmetrically, the thrust deviation angle becomes smaller as forces affecting the ramp tabs are offset in a proportionate manner. They consequently do not have significant impact on the entire thrust. When the ramp tabs are installed asymmetrically, side force is not offset, increasing in proportion to R1.

(c) Normal shock is nonexistent at a taper half angle of 5°, but at 14°, normal shock that can induce side force is generated. This normal shock is stronger when ramp tabs are installed asymmetrically than otherwise. Therefore, ramp tabs should be installed asymmetrically for enhanced thrust vector control over an aircraft.

5. REFERENCES

1) Kyoung Rean Kim et al., 2007, "A Performance Study and Conceptual Design on the Ramp Tabs of the Thrust Vector Control", transactions of KSME spring meeting, pp. 3068~3073.

2) Christopher M. Gourlay., "The Flow-Field Generated By Inclined Ramp Tabs In a Rocket Nozzle Exhaust", Univ. of Queensland, PhD Thesis, 1988.

3) J. M. Simmons, C. M. Gourlay and B. A. Leslie., "The Flow Generated by Ramp Tabs in a Rocket Nozzle Exhaust", AIAA 86-0282, 1986.

4) Deans, Arnold., "A Roket Vehicle", WO 82/01745 May, 1982.

5) Christopher P. Rahaim et al., "Jet Vane Thrust Vector Control : A Design Effort", AIAA 96-2904, 1996.